Repair of bone defects using synthetic mimetics of collagenous extracellular matrices

Matthias P. Lutolf[1,2], Franz E. Weber[3], Hugo G. Schmoekel[4], Jason C. Schense[5], Thomas Kohler[1], Ralph Müller[1], and Jeffrey A. Hubbell[1,2*]

Published online 21 April 2003; doi:10.1038/nbt818

We have engineered synthetic poly(ethylene glycol) (PEG)–based hydrogels as cell-ingrowth matrices for *in situ* bone regeneration. These networks contain a combination of pendant oligopeptide ligands for cell adhesion (RGDSP) and substrates for matrix metalloproteinase (MMP) as linkers between PEG chains. Primary human fibroblasts were shown to migrate within these matrices by integrin- and MMP-dependent mechanisms. Gels used to deliver recombinant human bone morphogenetic protein-2 (rhBMP-2) to the site of critical-sized defects in rat crania were completely infiltrated by cells and were remodeled into bony tissue within five weeks. Bone regeneration was dependent on the proteolytic sensitivity of the matrices and their architecture. The cell-mediated proteolytic invasiveness of the gels and entrapment of rhBMP-2 resulted in efficient and highly localized bone regeneration.

Although autologous bone grafts are routinely used to heal large bone defects, the disadvantages of this intervention (e.g., limited graft quantity, donor site morbidity) continue to drive the development of improved methods for bone regeneration. A promising alternative to autografting is the delivery of osteoinductive growth factors, such as members of the BMP family. BMPs, powerful regulators of many cell functions both in the embryonic and adult organism[1], are capable of forming *de novo* bone by acting on osteoprogenitor cells and inducing them to differentiate into mature osteoblasts[2,3]. Recombinant human forms of these proteins have been produced[4], and some BMPs, in particular BMP-2 and BMP-7, have been shown to induce bone formation in various animal models and in a recent human clinical study[5].

The efficient clinical use of BMPs depends critically on the delivery strategy: when administered in solution, BMPs will be rapidly cleared, resulting in suboptimal healing. The use of biomaterials that can retain and sequester BMPs greatly enhances efficacy and reduces protein dose by localizing the morphogenetic stimulus[6–8].

Both naturally derived and synthetic materials have been extensively tested as BMP carriers for bone regeneration. Collagen can bind BMPs to some degree and is readily infiltrated and remodeled into bony tissue[9,10]. However, like other natural polymers, it has some limitations in clinical use, primarily because of handling problems, the difficulty of engineering its properties, and its immunogenicity[11,12]. Among the synthetic BMP carriers, hydrolytically degrading polymers made from lactide and glycolide monomers have been applied most frequently. These traditional polymers can be problematic because they acidify and can form proinflammatory fragments upon degradation[13–16]. New formulations of these and related bulk-degrading polymers[17–20] may overcome some of these problems.

With very few exceptions, the design of synthetic biomaterials used for bone regeneration has been based upon structural and biomechanical criteria and upon passive mechanisms of growth factor delivery. The complex biological molecular interactions between cells and the extracellular matrix (ECM) have been largely ignored. The goal of this work was to develop a class of synthetic materials—designed on the basis of biological recognition principles[21–25]—that could mimic some of the key characteristics of biologically derived components of the ECM, such as collagen. Besides providing structural and biochemical cues for cells in contact, an important characteristic of the ECM is its susceptibility to cell-triggered proteolysis, which enables cell invasion and subsequent remodeling of the matrix, leading to regeneration[26]. At least three members of the MMP family[27,28]—MMP-2, MMP-9, and MT1-MMP—have been reported to play a major role in bone development and remodeling[28,29].

To mimic MMP-mediated matrix turnover, we engineered synthetic hydrogels containing a combination of crosslinking MMP substrates and pendant adhesion sites. Using *in vitro* and *in vivo* assays, we demonstrate that these bioactive networks can undergo cell-mediated proteolytic degradation, leading to further remodeling into a cell-secreted bone matrix at the site of an injury. Analysis of bone healing in a critical-sized defect in the rat calvarium by microcomputed tomography showed that our biomimetic matrix performed as well as bovine collagen matrix with regard to the degree of closure, bone volume, and bone connectivity (at 5 μg BMP-2 per defect). Thus, it was possible to mimic the invasion-conducting capacity of collagen without the use of the xenogeneic bovine protein carrier and its associated immunological complexities.

Results and discussion

Newly developed biomaterials intended for clinical use should be easy to handle and suitable for *in situ* application. Toward this end, we developed a synthesis scheme based on conjugate addition reactions between conjugated unsaturations on end-functionalized PEG macromers and thiol-bearing peptides that allows formation of

[1]*Institute for Biomedical Engineering, Swiss Federal Institute of Technology, Zurich and University of Zurich, Zurich, Switzerland.* [2]*Department of Materials Science, Swiss Federal Institute of Technology, Zurich, Zurich, Switzerland.* [3]*Department of Cranio-Maxillofacial Surgery, University Hospital Zurich, Zurich, Switzerland.* [4]*Small Animal Surgery, University of Bern, Bern, Switzerland.* [5]*Straumann, Biologics Division, Waldenburg, Switzerland.* **Corresponding author (hubbell@biomed.mat.ethz.ch).*

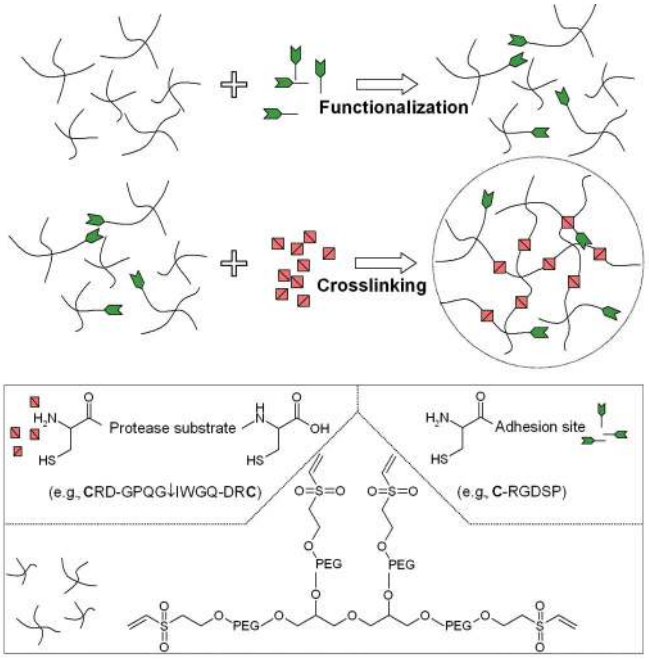

Figure 1. Scheme for gel preparation. Gel preparation procedure by selective conjugate addition. First a mono-functional peptide containing an integrin-binding RGDSP ligand for cell adhesion is reacted pendantly with a precursor containing multi-armed end-functionalized PEG macromers. Then the crosslinking is performed by the use of a bifunctional peptide. The bifunctional peptide determines the response of the material in the presence of cell-secreted enzymes, in this case, MMPs. As a result, these building blocks lead to the formation of elastic gel networks, to which cells can adhere, and which degrade to soluble products upon exposure to MMPs by cleavage of the crosslinking peptides.

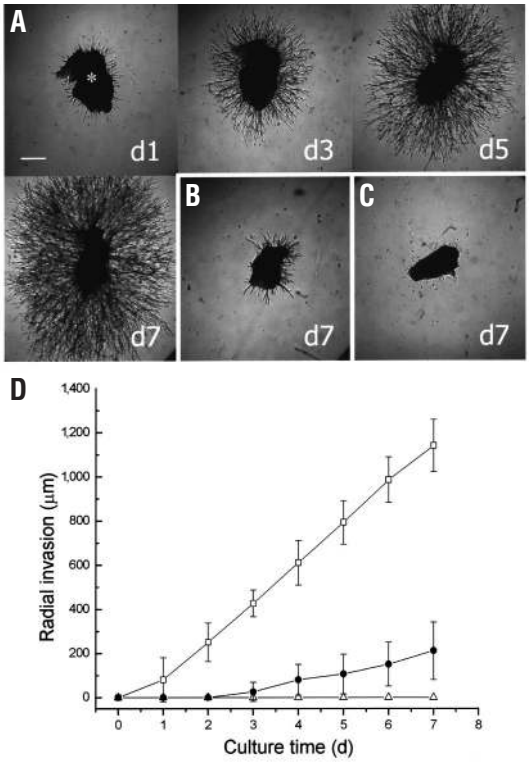

Figure 2. Three-dimensional fibroblast migration. (A) Fibroblasts migrate out in three dimensions from a cell-fibrin cluster (marked with *) into adhesive and MMP-sensitive synthetic matrices (corresponding to 1, 3, 5 and 7 d of culture of the same sample; □ in D). Cell invasion distances increase approximately linearly with culture time up to one week (n = 9–12). (B) In the presence of a broad-spectrum MMP inhibitor, hFF invasion was significantly reduced ($P < 0.01$) (day 7; ● in D), indicating that proteolysis was the main factor responsible for the outgrowth of cells. (C) Adhesion ligands were necessary for invasion to occur (day 7; △ in D). (D) Radial invasion of fibroblasts. Scale bar, 200 μm.

bioactive networks by the mixing of aqueous buffered solutions under almost physiologic conditions (Fig. 1).

***In vitro* fibroblast invasion.** We investigated the sensitivity of the gels to proteolysis by cell-secreted MMPs using an *in vitro* model system for cell invasion. Clusters consisting of primary human foreskin fibroblasts (hFFs) entrapped in a fibrin matrix were polymerized within PEG gels, and three-dimensional (3-D) outgrowth was assessed microscopically. Spindle-shaped fibroblasts migrated radially out from clusters into the surrounding PEG matrix at an invasion rate of approximately 7 μm/hour (Fig. 2). Invasion was absent, as expected, within networks lacking the RGD ligand or containing an inactive RDG control motif (Fig. 2C), as a result of the lack of biological recognition of PEG[30]. Based on swelling measurements, the network mesh size (indicative of the distance between consecutive crosslinks) of these networks was approximately 30–50 nm, that is, well below the dimensions of cellular processes. Thus, 3-D migration was limited to mechanisms involving proteolytic degradation. Indeed, very little or no invasion was observed when a broad-spectrum MMP inhibitor was added to the culture medium (Fig. 2B,D). Outgrowth was similarly hindered in gels composed of a crosslinking peptide without an MMP substrate, providing additional evidence that the synthetic matrix was predominantly degraded by cell-associated MMPs.

Release of rhBMP-2 from MMP-sensitive PEG gels and collagen sponges. In developing gels as carriers for BMP-2, we noted that the kinetics of protein release can greatly influence bone regeneration. Therefore, we studied the release of rhBMP-2 from synthetic PEG-based matrices *in vitro* using previously described methods[31], and compared it with release from a widely used collagen sponge (Helistat). Collagen retained ~85% of the absorbed 5 μg rhBMP-2 after 12 hours and 60% after 60 hours of washing, with rhBMP-2 continuing to be released at that time (Fig. 3). By contrast, synthetic PEG-based gels retained ~90% of the protein after 60 hours of incubation and the release curve had already leveled off after ~24 hours. The solubility of rhBMP-2 in physiological saline at pH 7.4 is relatively low, ~60 μg/ml[32], and it may be that this relatively low solubility in combination with the PEG present in the gel network keep the protein in a precipitated state until gel dissolution[32–34]. As the size limit for diffusion in these networks substantially exceeds the Stokes' radius of rhBMP-2, it seems unlikely that protein diffusion is physically hindered. It is also unlikely that the rhBMP-2 becomes covalently coupled to the gel, because the crosslinking reaction has been demonstrated to be highly selective[35]. Importantly, the release of the entrapped rhBMP-2 from the PEG networks was achieved upon exposure to MMP-2 (Fig. 3), mimicking the proteolytic activity associated with invading cells. This suggests that local proteolytic activity released entrapped rhBMP-2 from the gel matrix.

Healing of critical-size rat calvarial defects. We tested the synthetic hydrogel matrices in critical-size calvarial defects of the rat (with 5 μg rhBMP-2 per implant volume of 100 μl). After five weeks, animals were killed, and harvested cranial samples were analyzed histologically (Fig. 4A–D) and by microcomputed tomography (Figs. 4E,F and 5). Synthetic hydrogels that were adhesive and MMP-sensitive and that contained rhBMP-2 showed intramembranous bone formation (calcified bone stained in green with Goldner Trichrome) and osteoblasts (fuschia) at the osteoid interface between the newly deposited calcified bone and the fibroblast-like cells initially infiltrating the matrix

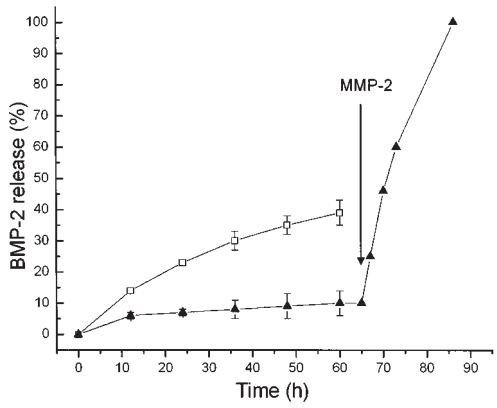

Figure 3. rhBMP-2 release triggered by MMP activity. Retention of physically entrapped and adsorbed rhBMP-2 (5 μg per 100 μl sample) in PEG gels (▲) and collagen sponges (□), respectively ($n = 5$). In contrast to collagen, PEG gels retain the protein almost completely (~90% after 60 h), most likely as a result of precipitation of the poorly soluble protein. Upon addition of exogenous active MMP-2, gels are degraded and the protein is released ($n = 1$), mimicking the cell-controlled release of the morphogen that can also occur *in vivo*.

(Fig. 4C). Gel formulations that lacked either rhBMP-2 (Fig. 4A) or MMP sensitivity (Fig. 4B) showed substantially less cell infiltration and bone formation. rhBMP-2 administration in Helistat collagen sponges, used as a positive control, led to bridging of bone that was histologically similar to that in the MMP-sensitive, rhBMP-2–bearing synthetic matrices, except that more bone seemed to be present in the center of the implant in the synthetic matrix (Fig. 4C,D). Whereas considerable amounts of residual collagen remained in the implant at five weeks (Fig. 4D), no residual synthetic matrix was found in any animal (Fig. 4C), demonstrating that complete matrix remodeling can occur without negative consequences to the newly formed bone.

We used microcomputed tomography to quantitatively analyze the cranial samples (Figs. 4E,F and 5). Calculations were made of the volume of bone in the defect, the connectivity of that bone, and the coverage of the defect with new bone by a pseudo-X-ray image obtained by calculating a projected image (in superior-inferior direction) from the 3-D microtomographic data set (Fig. 4E). By measures of bone volume and bone coverage, both MMP sensitivity ($P < 0.03$ for bone volume and $P < 0.02$ for bone coverage) and the presence of rhBMP-2 ($P < 0.01$ for both) were necessary to obtain good healing, similar to that with collagen sponges and rhBMP-2 ($P > 0.5$ for both). Although both histological and microtomographic imaging was qualitatively suggestive of higher connectivity in the bone formed in the MMP-sensitive, rhBMP-2–bearing synthetic matrix than in rhBMP-2–bearing collagen matrices (Fig. 4C,D,F), this trend did not show a high level of statistical significance ($P = 0.08$; Fig. 4E). Three-dimensional microtomographic projections (Fig. 4F) and two-dimensional serial sections (Fig. 5) were particularly revealing of the morphology of the healed bone.

The influence of cell-triggered matrix degradation on the healing outcome was most obvious when the crosslink density of the materials was changed by forming gels with different PEG macromers, namely 4armPEG-15 kDa (Fig. 6A) as contrasted with the 4armPEG-20 kDa (Fig. 6B) used in the measurements described above (corresponding to a change in volumetric swelling ratio of ~50%). The RGD ligand density and the MMP-sensitive peptide were not changed. Microcomputed tomography demonstrated equivalent coverage of the defect with bone in both cases, but higher bone volume in the 4armPEG-20kD matrix (Fig. 6C,D). In the more densely crosslinked network, bone formation was limited to the

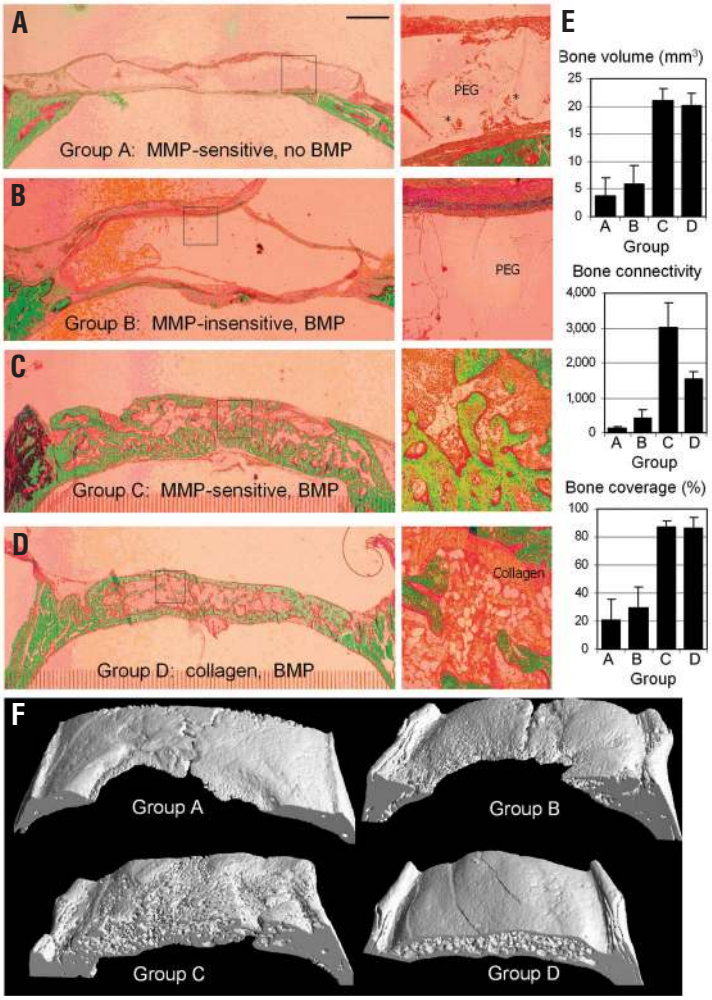

Figure 4. Bone healing in rat calvaria. Healing of critical-size rat calvarial defects five weeks after implantation ($n = 5$). (A–F) The ability of various matrices to promote healing was assessed by histology (A–D; scale bar, 1 mm) and microcomputed tomography (quantitatively in E, 3-D perspective in F). Quantitative healing indices were derived from microcomputed tomography measurements, namely bone volume (mm^3 of new bone in the defect), bone connectivity (see Experimental Protocol), and bone coverage of the defect (from a pseudoradiograph, reconstructed from the high-resolution microcomputed tomography images). In the synthetic matrices, the presence of rhBMP-2 and the enzymatic sensitivity of the matrix were critical for good healing: gels without physically entrapped rhBMP-2 (A) showed significantly less bone formation ($P < 0.01$ for bone volume, bone connectivity, and bone surface), as did gels that were not susceptible to degradation by proteases (B) ($P < 0.03$ for bone volume, 0.02 for connectivity, 0.02 for bone surface). In both of these specimens, large regions of noninfiltrated matrix (PEG) could still be found. Invasion of cells was observed in some areas (marked with *) of the MMP-sensitive matrix without rhBMP-2. MMP-sensitive and adhesive PEG gels that contained 5 μg rhBMP-2 promoted very good healing of the defects (C). New bone with bony trabeculae and developing marrow was formed. As determined by microcomputed tomography, the healing provided by this synthetic material was not statistically different from the widely used collagen sponges (D), ($P > 0.50$ for bone volume and bone surface). However, the histology and the 3-D renderings from microcomputed tomography are suggestive of higher bone connectivity in specimens treated with the synthetic matrix with rhBMP-2 than with a collagen sponge with rhBMP-2 ($P = 0.08$). Histological sections of representative samples were selected. Microcomputed tomographic reconstructions of animals with median bone volume were selected.

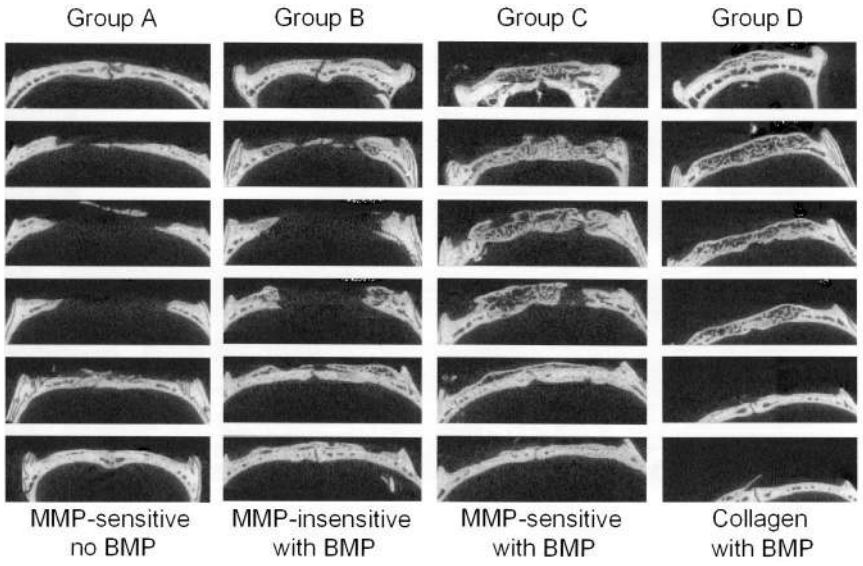

Figure 5. Micro-CT imaging of bone healing. Serial two-dimensional sections of microcomputed tomography of cranial samples of median bone volume. The requirement for both MMP-sensitivity and rhBMP-2 presence (Group C) can be clearly observed (Group A lacks MMP-sensitivity, and Group B lacks rhBMP-2 presence). Animals treated with collagen and rhBMP-2 (Group D) qualitatively demonstrated higher bone density close to the bone-tissue interface than animals treated with the synthetic matrix with rhBMP-2.

material interface with the dura, whereas it penetrated into the depths of the matrix in the 4armPEG-20kD, MMP-sensitive, adhesive matrix in the presence of rhBMP-2. Thus the gel architecture (here, crosslink density) had a profound influence on the speed of cell-triggered enzymatic remodeling.

It was reported that healing of bony tissue with Helistat sponges depends on the pharmacokinetics of BMP release[8]. Helistat is a fibrillar collagen sponge with pores up to several hundreds of micrometers in size. The porosity thus permits rapid cell infiltration without the need for enzymatic degradation. In contrast, our synthetic PEG-based gels require MMP-mediated degradation for cell invasion. We used this activity to locally trigger rhBMP-2 release with the aim of inducing a more localized healing response. This may be especially important in human applications, where larger doses of BMPs are required, and could also be an advantage when BMPs are applied in regions prone to heterotopic ossification, such as the hip or shoulder joints[36]. Indeed, concerns of heterotopic ossification were expressed by the European Agency for the Evaluation of Medicinal Products in its opinion of a product based on BMP-7 delivered in collagen particles derived from bovine bone[37]. Moreover, in the trial considered in this opinion, 10% of patients developed antibodies against BMP-7 and 5% developed antibodies against collagen[5], and this was of significant concern to the regulatory authorities[37]. The immunological benefits of a synthetic matrix compared with a biological one may be substantial. Although it is possible to develop antibodies directed against peptides, it is difficult to do so against peptides as small as the ones we use without conjugating them to larger antigenic species.

The biomimetic matrices described here combine the advantages of synthetic materials and of native protein-based materials such as collagen. Each component of the system can be reproducibly synthesized by chemical means with no risk of disease transmission. The biological efficacy of each component can be independently modulated in a defined way, starting from a passive background (PEG) that is not involved in signaling. The network architecture can be tailored by altering the functionality and molecular weight of PEG macromers. We have demonstrated in this report that such gels are suitable matrices to induce bone regeneration *in situ*. The applied synthesis scheme is rather adaptable, so in principle thiol-containing peptides and proteins of any structure or function can be incorporated. These materials should be useful in many tissue engineering applications and also in more fundamental studies of cell-matrix interactions.

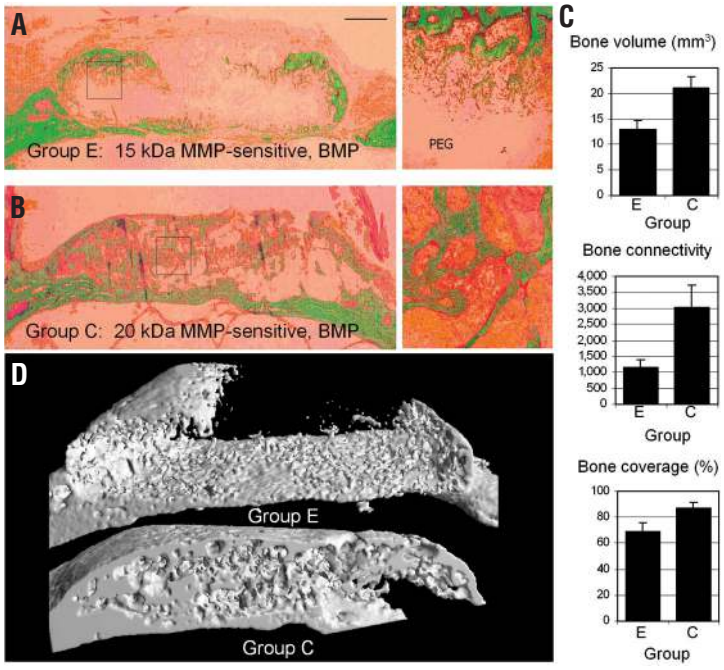

Figure 6. Effect of gel architecture. Healing depended on the hydrogel architecture. (A–D) MMP-sensitive and RGD-functionalized gels composed of 4armPEG-15 kDa (A) and 4armPEG-20 kDa (B) did not show significant differences with regard to bone coverage (C), but morphological differences were clearly apparent from histology and microcomputed tomography (D), which showed that infiltration was much more extensive in the synthetic matrices of lower crosslink density.

Experimental protocol

Materials. Branched PEGs (4arm PEG, 10 kDa; 4arm PEG, 20 kDa) were purchased from Shearwater Polymers (Huntsville, AL). Divinylsulfone was purchased from Aldrich (Buchs, Switzerland). Details of how branched PEG vinylsulfones were produced and characterized are available upon request from authors. All peptides (synthesis chemicals from Novabiochem, Läufelfingen, Switzerland) were synthesized on solid resin using an automated peptide synthesizer (PerSeptive Biosystems, Farmington, MA) with standard F-moc chemistry. Purification was performed by C18 chromatography (Biocad 700E; PerSeptive Biosystems) and peptides were analyzed by matrix-assisted laser desorption ionization/time-of-flight (MALDI-TOF) mass spectrometry. Collagen sponges (Helistat) were purchased from Integra Life Sciences Corporation (Plainsboro, NJ). Helistat is a crosslinked atelopeptide product composed of type I collagen, derived from bovine Achilles tendon.

Formation of PEG-based hydrogels. The synthesis of hydrogels was accomplished through Michael-type addition reaction[38] of thiol-containing peptides onto vinylsulfone-functionalized PEG. A typical adhesive and MMP-sensitive gel of 50 μl volume containing 10% (w/w)

PEG was formed by dissolving 5 mg PEG in 20 µl triethanolamine buffer (0.3 M, pH 8.0) and reacting this solution with 10 µl of 1 mM RGD (Ac-GCGYG*RGDSP*G-NH_2) in a first step. This solution was then mixed with 10 µl of a precursor solution (in the same buffer) containing a peptide with an MMP substrate (Ac-GCRD-GPQGIWGQ-DRCG-NH_2) or an MMP-insensitive control sequence (Ac-GCRD-GDQGIAGF-DRCG-NH_2) flanked by charged amino acids (Arg-Asp) and two Cys residues to render it more soluble and allow formation of a network, respectively.

Cell culture and 3-D cell invasion assay. Human foreskin fibroblasts (neonatal normal human dermal fibroblast; Clonetics, San Diego, CA) were grown in fibroblast cell culture medium (Dulbecco's Modified Eagle's Medium, with 10% fetal bovine serum and 1% antibiotic-antimycotic; Gibco-BRL, Life Technologies, Grand Island, NY) at 37 °C and 5% CO_2. A cell invasion assay was used according to a previously published method[24] in which hFF clusters within fibrin clots were embedded inside 10 µl hydrogel discs by placing a cluster into the precursor solution before gelation. Cell invasion was imaged (inverted phase contrast microscopy, Zeiss Axiovert 135, Zeiss (Feldbach, Switzerland)) and quantified with their center plane in focus (n = 9–12 per group).

rhBMP-2 preparation and release study. rhBMP-2 was prepared as described previously[36]. 5 µg rhBMP-2 was physically entrapped into PEG gels by mixing it with the PEG precursor before gelation. Helistat sponges were loaded with 5 µg rhBMP-2 by absorbing a solution (0.1 mg/ml) into a sponge strip and incubating for 1 h at 37 °C. rhBMP-2 release from both materials was studied based on a previously described method[31]. Samples were placed in 1 ml of TBS (pH 7.4) and stored at 37 °C and 100% humidity. The buffer was replaced every 12 h and refrigerated for further analysis. Finally, four synthetic gels were degraded with MMP-2 (10 nM; Oncogene, Reinbach, Switzerland) at different time points and the amounts of rhBMP-2 in the washes and degraded gels were analyzed using a Bio-Dot SF microfiltration apparatus (Bio-Rad, Hercules, CA) with a slot-blot device. In some experiments, a 25 µm GM6001 (Chemicon, Hofheim, Germany) was added as an MMP inhibitor.

Rat cranial surgery. Eight-millimeter diameter craniotomy defects were created with a trephine in a dental handpiece, carefully avoiding dural perforation. The surgical area was flushed with saline to remove bone debris and a preformed gel was placed within the defect. The soft tissues were closed with skin staples. Rats were killed by CO_2 asphyxiation five weeks after gel implantation. Craniotomy sites with 5 mm contiguous bone were recovered from the skull and placed in 40% ethanol. Twenty-five animals were randomly divided into five groups: 4PEG20-MMP(W)$_X$-RGD + 0 µg rhBMP-2 (Group A), 4PEG20-(DF)$_X$-RGD + 5 µg rhBMP-2 (Group B), 4PEG20-MMP(W)$_X$-RGD + 5 µg rhBMP-2 (Group C), 4PEG15-MMP(W)$_X$-RGD + 5 µg rhBMP-2 (Group E), Helistat (collagen) sponges + 5 µg rhBMP-2 (Group D). Abbreviations: 4PEG15/20 corresponds to the macromers 4armPEG-VS 15 kDa and 20 kDa, respectively. MMP(W)$_X$ corresponds to the MMP-sensitive peptide Ac-GCRD-GPQGIWGQ-DRCG-NH_2 bearing the Trp-containing MMP substrate (GPQGIWGQ), (DF)$_X$ to the MMP-insensitive Ac-GCRD-GDQGIAGF-DRCG-NH_2. RGD corresponds to the peptide Ac-GCGYGRGDSPG-NH_2 with the integrin-binding sequence RGDSP. All animal experiments were evaluated and permitted by the Veterinary Authority of the Canton of Zurich according to Swiss Federal Law Nr. 152/1997.

Microcomputed tomography. Explants were analyzed by microcomputed tomography on a µCT 40 imaging system (Scanco Medical, Bassersdorf, Switzerland) providing an isotropic resolution of 18 µm. A constrained Gaussian filter was used to partly suppress the noise in the volumes. Mineralized bone tissue was segmented from nonmineralized tissue using a global thresholding procedure[39]. All samples were binarized using the same parameters for the filter width (1.2), the filter support (1), and the threshold (224; in permille of maximal image gray value, corresponds to an attenuation coefficient of 1.8 cm^{-1}). Bone connectivity expresses the total number of connections in the bone volume and was directly derived from the Euler number[40]. Bone coverage was calculated from a projection of the cranium in superior-inferior direction to create a high-resolution pseudoradiograph. Three-dimensional visualizations were created using in-house software for surface triangulation and rendering[39,41].

Histology. Samples were prepared for histology[31] and stained with toluidine blue O and Goldner Trichrome (Sigma, Buchs, Switzerland).

Statistics. Statistical analyses of the data were performed using Statview 4.5 (Abacus, Berkeley, CA). Comparative analyses were completed using an unpaired, nonparametric Mann-Whitney test at a 95% confidence level. Mean values and s.d. are shown.

Acknowledgments

Funding of this study was provided by the Swiss National Science Foundation (NFP46 grant 58681), the Swiss Federal Agency for Education and Science (01.0224), and the European Union Framework 5 Program (C5RD-CT-2000-00267). We thank A. Zisch and G. Raeber for helpful discussions.

Competing interests statement

The authors declare competing financial interests: see the Nature Biotechnology website (http://www.nature.com/naturebiotechnology) for details.

Received 23 September 2002; accepted 21 January 2003

1. Kingsley, D.M. What do BMPs do in mammals: clues from the mouse short-ear mutation. *Trends Genet.* **10**, 16–21 (1994).
2. Wozney, J.M. & Rosen, V. Bone morphogenetic protein and bone morphogenetic protein gene family in bone formation and repair. *Clin. Orthop.* **346**, 26–37 (1998).
3. Schmitt, J.M., Hwang, K., Winn, S.R. & Hollinger, J.O. Bone morphogenetic proteins: an update on basic biology and clinical relevance. *J. Orthop. Res.* **17**, 269–278 (1999).
4. Wozney, J.M. *et al.* Novel regulators of bone formation: molecular clones and activities. *Science* **244**, 1528–1534 (1988).
5. Fiedlaender, G.E. *et al.* Osteogenic protein-1 (bone morphogenetic protein-7) in the treatment of tibial nonunions. *J. Bone Joint Surg.* **83A**, 151–189 (2001).
6. Li, R.H. & Wozney, J.M. Delivering on the promise of bone morphogenetic proteins. *Trends Biotechnol.* **19**, 255–265 (2001).
7. Brekke, J. & Toth, J. Principles of tissue engineering applied to programmable osteogenesis. *J. Biomed. Mat. Res.* **43**, 365–373 (1998).
8. Uludag, H. *et al.* Implantation of recombinant being bone morphogenetic proteins with biomaterial carriers, a correlation between protein pharmacokinetics and osteoinduction in the rat ectopic model. *J. Biomed. Mater. Res.* **50**, 227–238 (2000).
9. Boyne, P.J. Animal studies of application of rhBMP-2 in maxillofacial reconstruction. *Bone* **19**, 83–92 (1996).
10. Hollinger, J.O. *et al.* Recombinant human morphogenetic protein-2 and collagen for bone regeneration. *J. Biomed. Mater. Res. (Appl. Biomater.)* **43**, 356–364 (1998).
11. Ellingsworth, L.R., DeLustro, F., Brennan, J.E., Sawamura, S. & McPherson, J. The human immune response to reconstituted bovine collagen. *J. Immunol.* **136**, 8877–8882 (1986).
12. DeLustro, F., Dasch, J., Keefe, J. & Ellingsworth, L. Immune responses to allogeneic and xenogeneic implants of collagen and collagen derivates. *Clin. Orthop.* **260**, 263–279 (1990).
13. Boestman, O. Foreign-body reactions to fracture fixation implants of biodegradable synthetic polymers. *J. Bone Joint Surg.* **73B**, 592–596 (1990).
14. Meikle, M.C. *et al.* Effect of poly DL-lactide-co-glycolide implants and xenogeneic bone matrix-derived growth factors on calvarial bone repair in the rabbit. *Biomaterials* **15**, 513–521 (1994).
15. Kenley, R. *et al.* Osseos regeneration in the rat calvarium using novel delivery systems for recombinant human bone morphogenetic protein-2 (rhBMP-2). *J. Biomed. Mater. Res.* **28**, 1139–1147 (1994).
16. Zegzula, D., Buck, D.C., Brekke, J., Wozney, J.M. & Hollinger, J.O. Bone formation with use of rhBMP-2 (recombinant human bone morphogenetic protein-2). *J. Bone Joint Surg.* **79A**, 1778–1790 (1997).
17. Ertel, S.I. Evaluation of poly(d-carbonate), a tyrosine-derived degradable polymer, for orthopedic applications. *J. Biomed. Mater. Res.* **29**, 1337–1348 (1995).
18. Anseth, K.S., Sharstri, V.R. & Langer, R. Photopolymerizable degradable polyanhydrides with osteocompatibility. *Nat. Biotechnol.* **17**, 156–159 (1999).
19. Zhu, G., Mallery, S.R. & Schwendeman, S.P. Stabilization of proteins encapsulated in injectable poly(lactide-*co*-glycolide). *Nat. Biotechnol.* **18**, 52–57 (1999).
20. Saito, N. *et al.* A biodegradable polymer as a cytokine delivery system for inducing bone formation. *Nat. Biotechnol.* **19**, 332–335 (2001).
21. Hubbell, J.A. Bioactive biomaterials. *Curr. Opin. Biotechnol.* **10**, 123–129 (1999).
22. Griffith, L.G. & Naughton, G. Tissue engineering—current challenges and expanding opportunities. *Science* **295**, 1009–1014 (2002).
23. Pratt, A.B. & Hubbell, J.A. *Cell-responsive Synthetic Biomaterials Formed In Situ* (California Institute of Technology, Pasadena, CA, 2001).
24. Halstenberg, S., Panitch, A., Rizzi, S., Hall, H. & Hubbell, J.A. Biologically engineered protein-graft-poly(ethylene glycol) hydrogels: a cell adhesive and plasmin-degradable biosynthetic material for tissue repair. *Biomacromolecules* **3**, 710–723 (2002).
25. Gobin, A.S. & West, J.L. Cell migration through defined, synthetic ECM analogs. *FASEB* **16**, 751–753 (2002).
26. Clark, R.A.F. Molecular and Cellular Biology of Wound Repair (Plenum Press, NY, 1996).
27. Woessner, J.F. & Nagase, H. *Matrix Metalloproteinases and TIMPs* (Oxford Univ. Press, New York, 2000).
28. Sternlicht, M.D. & Werb, Z. How matrix metalloproteinases regulate cell behavior. *Annu. Rev. Cell Dev. Biol.* **17**, 463–516 (2001).
29. Vu, T.H. & Werb, Z. Matrix metalloproteinases: effectors of development and normal physiology. *Genes Dev.* **14**, 2123–2133 (2000).
30. West, J.L. & Hubbell, J.A. Separation of the arterial wall from blood contact using hydrogel barriers reduces intimal thickening after balloon injury in the rat: the roles of medial and luminal factors in arterial healing. *Proc. Natl. Acad. Sci. USA.* **93**, 13188–13193 (1996).
31. Weber, F.E., Eyrich, G., Graetz, K.W., Maly, F.E. & Sailer, H.F. Slow and continuous application of human recombinant bone morphogenetic protein *via* biodegradable poly(lactide-co-glycolide) foamspheres. *Int. J. Oral Maxillofac. Surg.* **31**, 60–65 (2002).
32. Ruppert, R., Hoffmann, E. & Sebald, W. Human bone morphogenetic protein 2 contains a heparin-binding site which modifies its biological activity. *Eur. J. Biochem.* **237**, 295–302 (1996).
33. Patel, S., Cudney, B. & MacPherson, A. Polymeric precipitants for the crystallinization of macromolecules. *Biochem. Biophys. Res. Commun.* **207**, 819–828 (1995).
34. Uludang, H. *et al.* rhBMP-collagen sponges as osteoinductive devices: effects of *in vitro* sponge characteristics and protein pi on *in vivo* rhBMP pharmacokinetics. *Ann. New York Acad. Sci.* **875**, 369–378 (1999).
35. Elbert, D.L., Pratt, A.B., Lutolf, M.P., Halstenberg, S. & Hubbell, J.A. Protein delivery from materials formed by self-selective conjugate addition reactions. *J. Contr. Rel.* **76**, 11–25 (2001).
36. Weber, F.E. *et al.* Disulfide bridge conformers of mature BMP are inhibitors for heterotopic ossification. *Biochem. and Biophys. Res. Commun.* **268**, 554–558 (2001).
37. European Agency for the Evaluation of Medicinal Products. European Public Assessment Report: osteogenic protein 1 (Cpmp/0393/01). *www.eudra.org/humandocs/humans/epar/osteogenicprot1/osteogenicprot1.htm* (2001).
38. Lutolf, M.P., Tirelli, N., Cerritelli, S., Cavalli, L. & Hubbell, J.A. Systematic modulation of Michael-type reactivity of thiols through the use of charged amino acids. *Bioconj. Chem.* **12**, 1051 (2001).
39. Muller, R. & Ruegsegger, P. Micro-tomographic imaging for the nondestructive evaluation of trabecular bone architecture. *Stud. Health Technol. Infor.* **40**, 61–79 (1997).
40. Odgaard, A. & Gundersen, H.J. Quantification of connectivity in cancellous bone, with special emphasis on 3-D reconstructions. *Bone* **14**, 173–182 (1993).
41. Muller, R., Hildebrand, T. & Ruegsegger, P. Noninvasive bone-biopsy—a new method to analyze and display the 3-dimensional structure of trabecular bone. *Phys. Med. Biol.* **39**, 145–164 (1994).